Investigation of Laser Induced Plasma Assisted Ablation of Glass in Presence of Magnetic Field

N. Abbasi[1], M. R. Razfar[1*], S. M. Rezaei[1], K. Madanipour[2], M. Khajehzadeh[1]

[1] Department of Mechanical Engineering, Amirkabir University of Technology, Tehran, Iran
[2] Department of Physics and Energy Engineering, Amirkabir University of Technology, Tehran, Iran

ABSTRACT: The present paper is devoted to the study of glass ablation with laser-induced plasma and the effect of the magnetic field on this process. In the experiments, a nanosecond pulsed laser with a wavelength of 532 nm and copper with 2 mm thickness is used as the laser source and the metal substrate respectively. Two permanent neodymium magnets (4500-4800 G) are used to apply an external magnetic field to the drilling zone and to make ablation on the laboratory slide glass. The laser fluence is selected in 4 levels of 1, 1.5, 3, and 3.5 J/Cm^2 and the characteristics of the holes made with 50 pulse laser radiation are compared in terms of dimensions and morphology. It is observed that by applying a magnetic field, the removed material volume increases about 2 to 2.4 times in the lower fluences and 31 to 35 times in the higher fluences. In the magnetic field absence, for different levels of laser fluence, depth and diameter are changed from 1.6 to 32 and 10 to 100 microns. However, in its presence, they are changed from 3 to 76 and 11 to 380 microns respectively. The shape of deposited particles on glass is also different in the presence and absence of a magnetic field.

1- Introduction

Due to its properties like electrical conductivity, high hardness, high chemical stability, corrosion resistance, corrosion conductivity, and low thermal deformation glass is one of the most widely used materials. Industries include Microelectronics [1], Optics [2-3], Optofluidic [4], Microfluidic equipment [5-6], Micro detectors [7], micro-pump, microreactor and micro-fuse [8-9]. However, the brittleness of this material makes its machinability to be low and it cannot be easily machined with conventional methods. Various new methods have been used for machining, drilling, or creating textures on glass [10]. Ultrasonic machining [11-12], abrasive water jet [13], electrochemical discharge machining process [14-17], wet and dry etching [18], and photolithography [19] are some of the new methods used for glass machining. But each of these methods has its own limitations. Meanwhile, laser-assisted machining especially in short-pulsed lasers plays a vital role in this field due to its unique properties. It is particularly useful due to its ability to machine a variety of conductive and non-conductive materials with a high aspect ratio and high-speed machining [20-22]. Based on this and considering the capabilities of laser light and its ease of use, it is a desirable option for the micromachining of many materials. However, glass is transparent to visible or infrared laser light, and machining with a direct laser beam is not easily possible. Precise micromachining of glass can be done with femtosecond lasers, but the low material removal rate and high cost of using these lasers are among the disadvantages

of this method. Nanosecond lasers, which are the most common lasers in the industry have low material removal rates at low energies and they damage the glass at high energies. Therefore about two decades ago, following the efforts of researchers to glass machining with nanosecond lasers and to find a solution for easier machining in less time, low cost, and higher quality; laser induced plasma-assisted ablation process without the need for special and complex tools or conditions was introduced. The schematic of this process is shown in Fig. 1.

Zhang et al. [23] have conducted micro-machined and micro grating of quartz and glass using laser-induced plasma ablation. A model was presented to explain the ablation mechanism and experimentally studied the depth of the crater created at various energies and different gaps between glass and substrate. In the other study [24], laser wavelength variation effects on the micro grating of silica were shown. It has been shown that the ablation rate decreases with increasing laser wavelength. Kadan et al. [25] have used ablation operations with laser-induced plasma for micro marking in sapphires, silica, and glass. Hanada et al. [26] have developed this ablation method for micromachining of glass at high-speed and creating complex structures. Likewise, this process has been used for polyamide selective metallization [27-28]. They have also shown that marking without cracks and color marking of glass with ablation is possible by using laser-induced plasma [29].

*Corresponding author's email: Razfar@aut.ac.ir
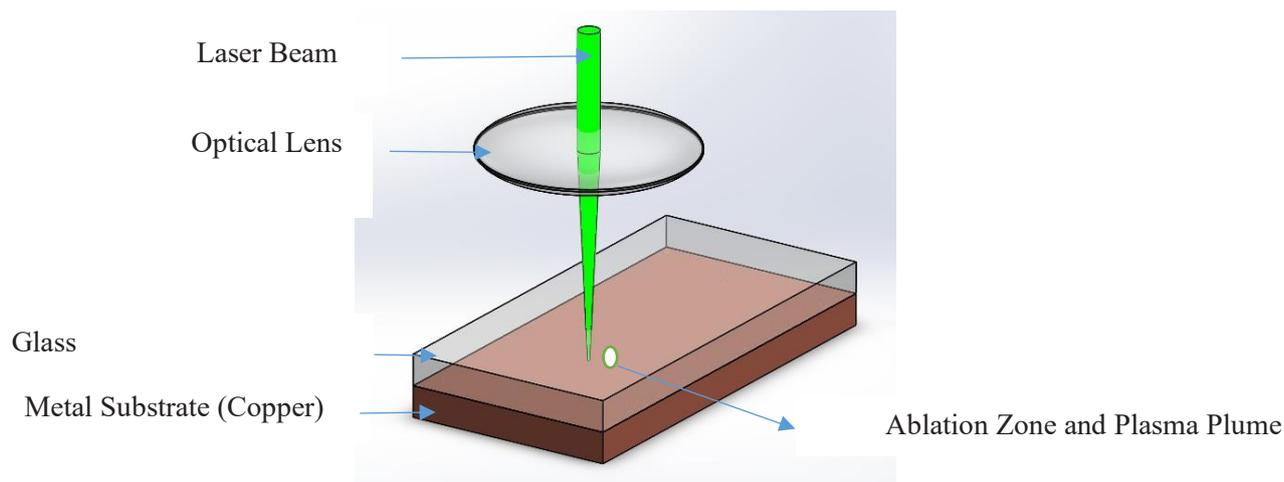
Fig. 1. Schematic of laser-induced plasma-assisted ablation and glass micromachining

Shujia et al. [30] have combined laser-induced plasma-assisted ablation and electroplating to enable the rapid and inexpensive fabrication of electro fluidic equipment. They have created a channel by using graphite as a substrate and a laser-induced plasma-assisted ablation process. As a result of this process, a graphite layer is deposited on the glass, and the adhesion strength and conductivity of the graphite particle coating are increased by electroplating nickel on the graphite. Rahman et al. [31], have investigated the effect of variation of laser energy on the plasma features and crater morphology produced by laser-induced plasma-assisted ablation process. Based on their results, by increasing the laser fluence, the crater depth, and its diameter increase. Also, as the distance between the glass and the target material increases, the crater depth and its diameter decrease linearly. Yu Zhao et al. [32] have created a microchannel on quartz by using an excimer laser and laser-induced plasma-assisted ablation. Their metal target was 304 stainless steel. According to their study, in this process, two phenomena of ablation stemming from laser-induced plasma and direct interaction between the laser and the glass occur simultaneously due to the deposition of metal particles behind the glass. By optimizing the parameters, they have enabled the creation of a channel up to a depth of 28 microns and surface roughness of several hundred nanometers. Sarma and Joshi [20] have studied the laser-induced plasma-assisted ablation parameters effects on the channel created on the glass. They have used an Nd:YAG laser and a wavelength of 1064 nm and have studied the effect of pulse duration, power peak of laser, and scanning speed on the channel width. They have shown that as the scan speed increases, the groove width decreases, and the continuous channel does not form at high speeds. The current Increasing from 50 to 80 amperes and pulse time increasing from 0.5 ms to 4 ms both increase the groove width.

As can be observed in the cited studies, the main goals of researchers in the laser-induced plasma-assisted ablation process were the optimization of the process parameters,

reducing costs, improving the quality of machining, and increasing the material removal rate.

Laser-induced plasma-assisted ablation uses the plasma generated from the laser-matter interaction and the plasma dynamics significantly affect the characteristics of the created hole [33-34]. Thus, the micro-machining conditions can be improved if the plasma can be controlled or its characteristics can be changed. Plasma is an ionized medium which contains charged particles, so if plasma develops in a magnetic field, the plasma dynamics will be significantly affected by the magnetic field.

In the literature, the magnetic field effect on micromachining with laser-induced plasma has been studied. Harilal et al. [35] have investigated the magnetic field confinement effect on laser-induced plasma. This study shows that the structure of the plasma and the dynamics of its evolution change by applying a magnetic field. Kondo et al. [36] have shown that the magnetic field applied to laser-generated plasma increases the ion beam current and the plasma shelf life. A similar magnetic field confinement effect has been studied by Pagano and Looney [37] and Lash et al. [38].

The effect of an external magnetic field on the process of drilling opaque materials with a laser has been investigated in some studies. Chang et al. [39] have investigated the effect of a magnetic field on the drilling of copper by the laser-induced plasma micromachining process, where 10 laser pulses with an energy of 110 mJ are irradiated on the copper surface in the presence and absence of a magnetic field. The results show that the hole depth is increased 1.75 times in the presence of a magnetic field compared to the absence of it. The taper angle of the hole also becomes sharper and decreases from 155 degrees which were created in the absence of a magnetic field, to 103.7 degrees in the presence of the magnetic field. Chang et al. [40] have used a magnetic field in the laser micro-drilling of 6061 aluminum which is highly reflective of laser light. Using a static magnetic field, the machining process

is increased several times in depth and the hole diameter is decreased by 42%. The circularity of the hole entrance is also improved. In these studies the second harmonic of the Nd:YAG laser has been used with a wavelength of 532 nm, pulse mode with a maximum energy of 270 mJ, and a pulse width of about 6 nanoseconds, and a frequency of 50 Hertz. Wolff and Saxena [41] have changed the number of magnets and the dielectric material and have created channels and holes on the metal piece. It has been shown that in the presence of the field, more machining depth can be achieved and the quality of channel geometry can be improved.

By careful analysis of previous studies, it can be observed that the process of laser-induced plasma-assisted ablation in the presence of a magnetic field has not been studied so far. As an innovation, the effect of an external magnetic field on the morphology and dimensional plus geometrical characteristics of the hole created on the glass by laser-induced plasma-assisted ablation is studied in the present paper. In the experiments, glass drilling is performed with four levels of laser fluence in the presence and absence of a magnetic field. The results are evaluated in terms of the amount of material removed from the glass surface, maximum diameter and maximum depth of the crater as well as metal spattering on the rear surface of the glass.

2- Process Theory Analysis

The analysis of this process is very difficult due to the complexity of the laser-matter interaction and the plasma-matter interaction. To understand this process a model is provided using some simplifications and assumptions to explain the process. Distinguishing the phenomena that take place during this process, it can be stated that with laser radiation, the laser beam passes through the glass and hits the metal surface at the interface between the glass and metal. When a laser beam with an intensity of several gigawatts per square centimeter strikes the metal surface, an initial ablation is occurred on the metal, and by ionizing the vaporized material from the metal surface, a plasma plume is formed before the laser pulse is turned off. Due to the plasma shielding effect, part of the laser energy is absorbed by the plasma and the plasma plume begins to expand. In this process, two confinement effects are applied to the plasma by the glass placed on the metal and the magnetic field on the surface, and the plasma is trapped in the area between the glass and the metal. Regarding the confinement of plasma with glass, with the absorption of laser energy by plasma, the plasma pressure increases and opens the interface causing a shock wave to be applied to glass and metal material [42]. After the laser pulse is turned off, the plasma maintains its pressure and by moving perpendicular to the magnetic field, a force is applied to the plasma plume from the field and an induced current is created inside the plume, which increases the internal energy of the plume and consequently leads to the increase of the plasma temperature. In general, to describe the motion of a fluid, it is necessary to obtain the equations of conservation of mass, energy, and momentum for it [43]. The mass conservation equation (Eq. (1)) is obtained using the mass balance in a

volumetric element that fluid is flowing in it. To obtain the equation of motion or the momentum (Eq. (2)) for a fluid, the motion balance for a volumetric element must be written. According to this equation, the rate of momentum increase is equal to the rate of momentum entering the volume element minus the rate of momentum leaving the volume element plus external forces. Eq. (3) is the energy conservation law. According to this law, the total rate of input and output energies, the rate of work done by the system or on the system through molecular transmission or by external forces, and the rate of energy production is zero. Now considering plasma as a fluid, if the hydrodynamic equations (Eqs. (1) to (3)) are written in the presence of a magnetic field, the expression $\vec{J} \times \vec{B}$ appears in the momentum equation (Eq. (2)) as a force exerted by the magnetic field, and the expressions $u(\vec{J} \times \vec{B})$ and $\frac{\left|\vec{J}\right|^2}{\sigma}$ appear as the work done by the force from the field and the effect of Joule heating, respectively, in the energy equation. In these relationships B is the intensity of the applied magnetic field, J is induced electrical current density, σ is electrical conductivity, and u is plasma velocity in the direction perpendicular to the magnetic field.

$$\frac{\partial \rho}{\partial t} + \frac{\partial (\rho u)}{\partial z} = \cdot \tag{1}$$

$$\frac{\partial (\rho u)}{\partial t} + \frac{\partial (\rho u^2 + P)}{\partial z} = (\vec{J} \times \vec{B}) \vec{a_z} \tag{2}$$

$$\frac{\partial (E + \frac{1}{2} \rho u^2)}{\partial t} + \frac{\partial \left[u(E + \frac{1}{2} \rho u^2 + P) \right]}{\partial z} =$$
$$\frac{\partial}{\partial z}(k \frac{\partial T}{\partial z}) + \frac{\partial I}{\partial z} + \frac{\left|\vec{J}\right|^2}{\sigma} + u(\vec{J} \times \vec{B}) \vec{a_z} \tag{3}$$

Accordingly, the plasma motion in any direction other than parallel to the magnetic field induces an electrical current in the plasma and a force will be applied to the plasma plume from the magnetic field. This force traps the plasma and slows plasma movement down. Plasma temperature and pressure increase as the plasma velocity slows down and the kinetic energy of the particles is converted to internal energy and the collisions of particles and plasma components inside the plume increase. Plasma, which absorbs a large part of the laser energy, can transfer a part of the energy to glass by various heat transfer mechanisms, such as conduction. With a simple and general estimate, the amount of heat transferred from the plasma to the workpiece can be obtained by the heat transfer equation ($Q = kA\Delta T$), where Q is the amount of energy transferred, k is the heat transfer coefficient, A is a cross-section, and ΔT is temperature difference between plasma and glass. It is known that the higher the plasma temperature has the more heat transfer between plasma and

Table 1. Chemical composition of soda ash glass [45]

Composition	SiO_2	Na_2O	CaO	MgO	Al_2O_3	K_2O
Wt , %	73	14	9	4	0.15	0.03
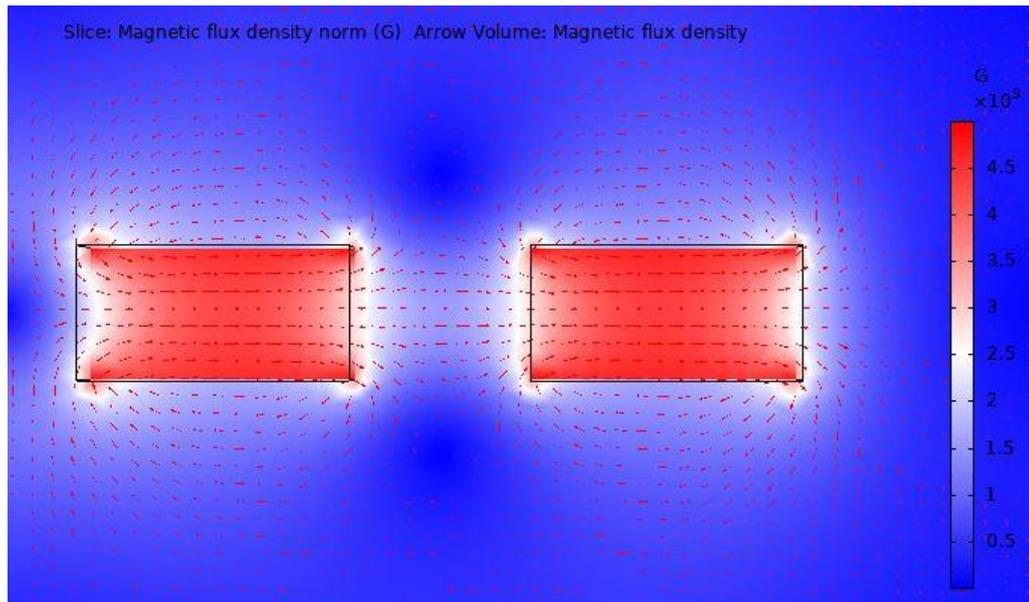
Fig. 2. View of magnetic field lines and magnetic field flux density applied by magnets

glass is. Plasma is an ionized state of a gas. The mechanism of conductive heat transfer in gases depends on molecular motion. The higher velocity of the molecules, the faster the heat transfer rate from one molecule to another; it indicates that the conduction heat transfer coefficient has increased. As the temperature increases, the plasma heat transfer coefficient increases [39, 44], which also helps to increase the amount of heat transferred to the glass and further increase the ablation from the glass surface. According to the existing relationships and the stated analyzes, the application of an external magnetic field should theoretically increase the material removal rate in the process.

3- Experimental Setup

In this study, the ablation on the laboratory glass slide is studied. The composition of the soda lime glass used for the experiment is given in Table 1. Copper is used as the metal substrate behind the glass. For maximum ablation, copper and glass are stacked without gaps. Q-switched Nd:YAG laser is used with a pulse duration of 12 ns, 532 nm wavelength, and 8 mm laser beam diameter. In the experiments, the metal (copper) and glass are first cleaned using ethanol and using

an ultrasonic cleaning device and then clamped together. To create a transverse magnetic field (perpendicular to the direction of laser radiation), 2 permanent neodymium magnets with dimensions of 50 × 30 × 15 mm with an intensity of 4500 to 4800 Gausses are used. The opposite poles of the magnets are placed facing each other at 2 cm from each other and the set of glass and copper is placed in the space between the magnets. Fig. 2 shows the magnetic field lines and magnetic field flux density generated by these magnets, which were plotted with the COMSOL Multiphysics software. It is observed that near each of the magnets and in the central part of each magnet, the density of magnetic field lines is higher, and the magnetic field is more uniform. Accordingly, and using the positioning table, the glass, and copper assembly is placed in a central position between the two magnets so that the highest flux density and uniformity of the magnetic field is obtained in the plasma formation zone. Also, magnetic field lines are applied parallel to the glass surface. The laser light irradiates onto the substrate surface. Also, the laser focal spot is at the interface between glass and copper and on the surface of copper. The schematic of the experimental setup and the location of the parts are shown in Fig. 3.
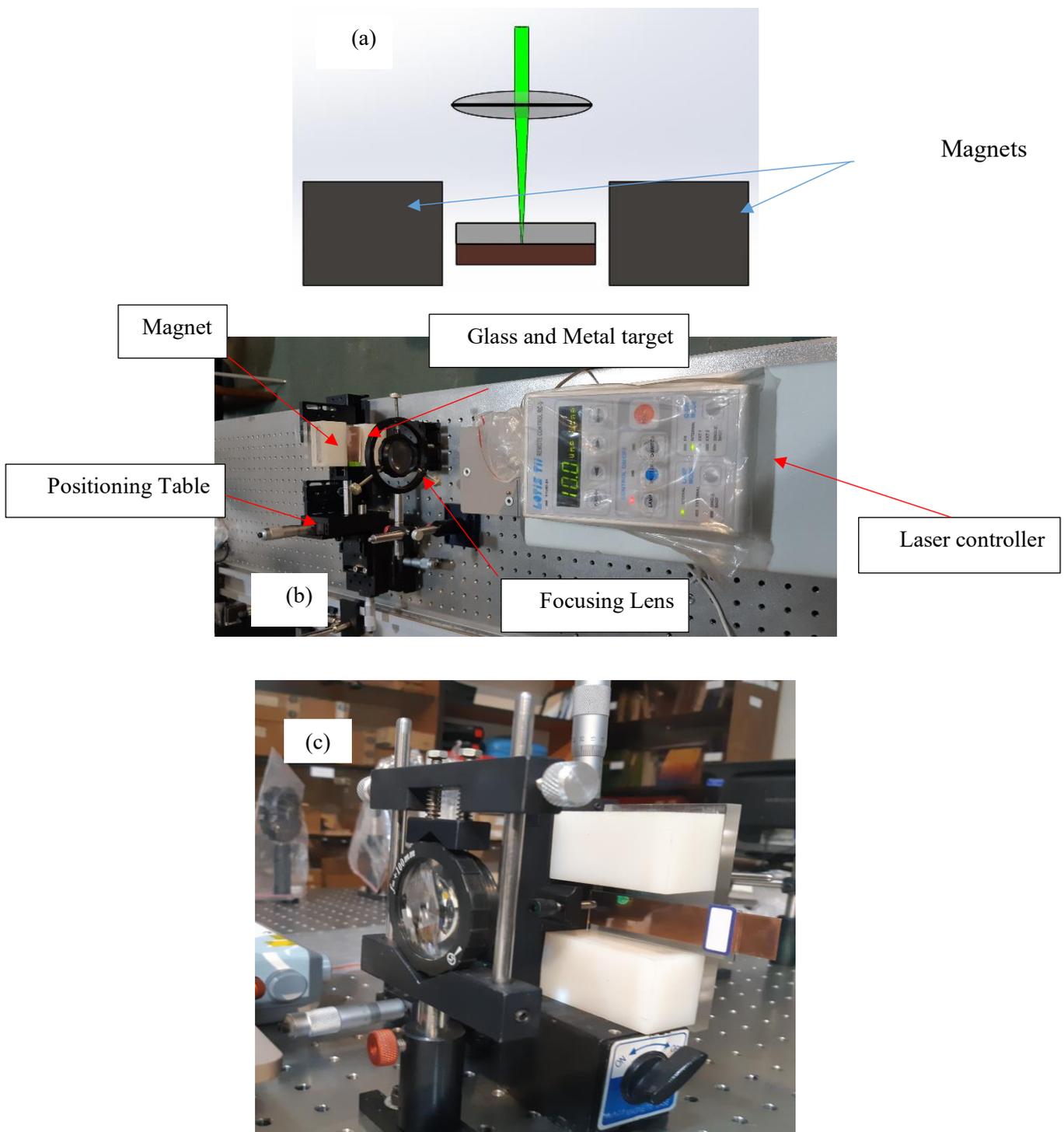
Fig.3. a) Schematic of Experimental setup, b) Experimental setup, c) Close view of the placement of metal, glass and magnets, and laser radiation

Table 2. Conditions of experimental tests

No.	Laser fluence J/cm^2	Pulse Number	Repetition rate Hz	Focal length mm	Description
1	1				
2	1.5				All experiments were performed in the
		50	10	50	presence and absence of an external
3	3				magnetic field.
4	3.5				

Table 3. Characteristics of the holes created in different test conditions

No.	Laser Fluence J/cm^2	Without Magnetic Field			With Magnetic Field		
		Max. Diameter μm	Max. Depth μm	Circularity	Max. Diameter μm	Max. Depth μm	Circularity
1	1	10	1.6	0.90	11	3	0.89
2	1.5	20	5.9	0.87	32	7.3	0.84
3	3	81	23	0.82	260	55	0.78
4	3.5	100	32	0.78	380	76	0.78

Laser machining parameters with and without an external magnetic field are selected according to Table 2. The laser beam is selected on the target material in a way that the laser intensity is higher than the threshold for plasma formation on copper and less than the threshold for direct glass breakdown or damage. For this purpose, initial tests are performed to determine the amount of laser intensity in the process and the appropriate interval of the mentioned parameter is determined.

To study the hole characteristics, samples are taken in copper etchant solution with a combined ratio of $H_2O_2:1, HCO_3H:18, H_2O:1$ at a temperature of 45°C and an etching rate of 1 micron per minute, etched to a layer of copper deposited on the surface of the glass. Then glass surface profilometry is performed. A spattering of materials in this process is evaluated by light microscopy before etching the glass.

4- Results and Discussion

4- 1- Hole depth and diameter

The holes produced on the glass by the laser-induced plasma-assisted ablation in the presence and absence of the magnetic field, after removing the deposited material in and around the holes, are studied. Surface profilometry is performed from the middle section of the cavities in one direction. The holes' profiles produced in experimental conditions are shown in Fig. 4. As shown in Fig. 4, the depth and diameter of the ablation increase by increasing the laser fluence. This is due to the more evaporation of the metal material and the formation of a larger plasma. Larger plasma absorbs more energy from the laser, resulting in higher temperatures and pressures, which leads to increased material removal in larger dimensions (in diameter and depth). The considerable point, which is shown in Table 3, is the diameter and depth of the holes created in the presence of
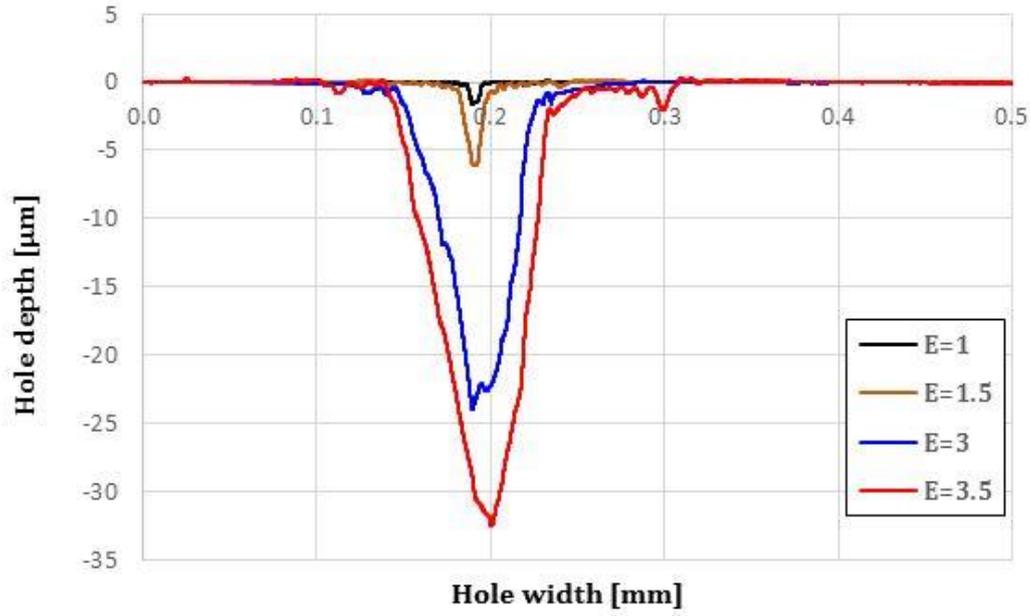
(a)
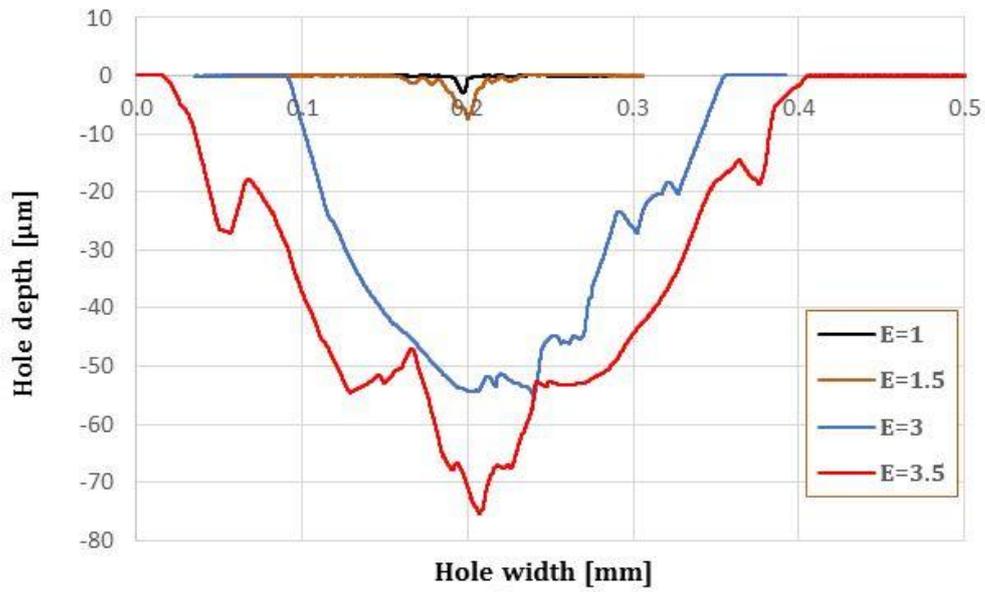
(b)

Fig. 4. Profiles of holes created with various energies a) in the absence of a magnetic field, b) in the presence of a magnetic field.
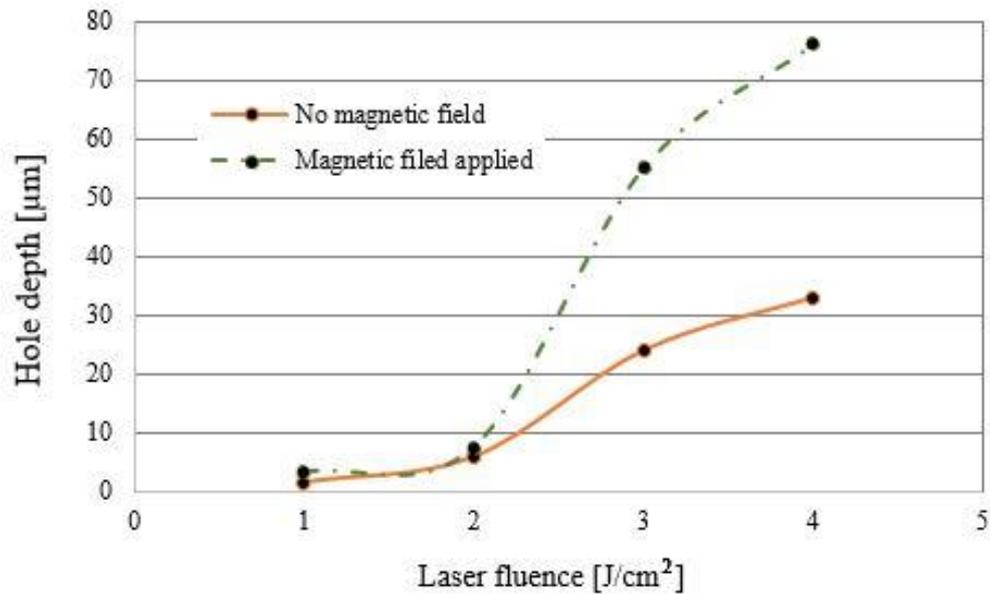
Fig. 5. Hole depth variation versus laser beam energy in the presence of a magnetic field (dashed line) and in its absence (filled line)

the magnetic field which is greater than those created without the magnetic field presence. In laser fluence $1_{J/Cm^2}$ in the absence of a magnetic field, the diameter of the hole is 10 microns with a maximum depth of 1.6 microns and in the presence of a magnetic field, the hole diameter is 11 microns with a depth of 3 microns. In laser fluence $1.5_{J/Cm}$, in the absence of a magnetic field, the hole diameter is 20 microns with a maximum depth of 5.9 microns and, in the presence of a magnetic field, they are 32 Microns and 7.3 microns, respectively. In laser fluence $3_{J/Cm}$, in the magnetic field absence, the hole diameter is 81 microns with a maximum depth of 23 microns and, in the magnetic field presence, the diameter and depth are 260 and 55 microns, respectively. When the laser fluence is $3.5_{J/Cm}$, the inlet diameter is about 100 microns and its maximum depth is 32 microns, when the magnetic field is applied, the diameter is 380 microns, and the maximum depth is 76 microns. It can be concluded that under the same machinating conditions, the diameter of the created hole in magnetic field presence is 3.2 times and its depth is 2.31 times greater than when there is no magnetic field.

By comparing the hole depths and diameters created in different energies, it is observed that the average inlet diameter is 2.4 times, and the maximum depth of the holes is 1.98 times greater when the magnetic field is present, and both of these ratios increase with the increase of laser energy.

Variation in the depth and diameter of the holes at different energies and in the presence/absence of the magnetic field is shown in Figs. 5 and 6. In the direction perpendicular to the glass surface, the plasma grows to a certain height and then turns off, but in the presence of a magnetic field, the plasma expands in the depth direction. Although the growth rate of

the plasma is reduced by Lorentz's force, the hole expands in the depth direction by conversion of kinetic energy into internal energy. Due to the reduction of velocity, joule heating effect, and induced current inside the plasma, as a result of movement in the direction perpendicular to the field, the internal energy of the plasma increases and leads to an increase in temperature and pressure of the plasma plume. Accordingly, a plasma with higher temperature and pressure is obtained in the ablation zone. Thus, the presence of a magnetic field increases the depth and diameter of the hole created. On the other hand, since the horizontal velocity of plasma is not affected by the magnetic field, the horizontal plasma velocity in both the presence and absence of the magnetic field is almost the same. Therefore, the ratio of increase in hole diameter is higher than the ratio of increase in hole depth. Also, at high energies where larger plasma is formed, the plasma is affected more by the magnetic field and there is a significant increase in plasma-assisted ablation.

4- 2- Hole circularity:
The circularity of the hole inlet diameter can be evaluated by the ratio of the minimum diameter to the maximum diameter of Fret at the hole entrance [21]. The diameter of the Fret is the distance between two parallel planes that are tangential to the hole profile. As the minimum to maximum diameter ratio becomes closer to 1, the hole inlet profile becomes closer to the circle. The holes' circularity produced in different laser fluences and in the presence of a magnetic field and without it is shown in Table 3. It is observed that the circularity decreases by increasing the laser energy or equivalently increasing the laser fluence. This is due to the increased melting and evaporation from the glass surface, which causes more
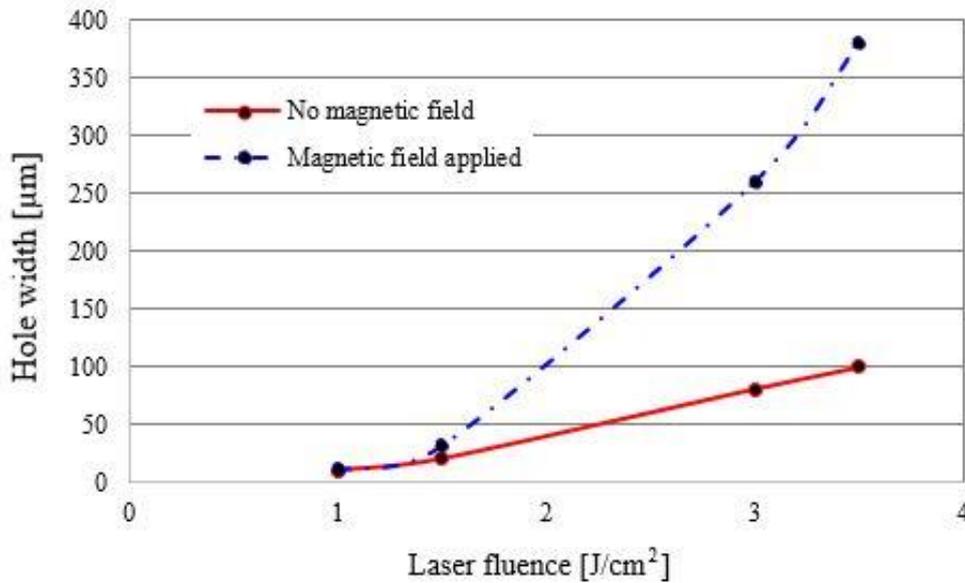
Fig. 6. Hole diameter variation versus laser beam energy in the presence of a magnetic field (dashed line) and in its absence (filled line)

irregularities at the inlet of the hole. Also, in most tests, by applying a magnetic field, the circularity is slightly reduced compared to when there is no magnetic field. This is due to the increase in temperature and pressure of the plasma in the presence of a magnetic field and because more heat is transferred to the target and the plasma is deformed due to the limited velocity of its particles in non-parallel directions in presence of the magnetic field.

4- 3- Material removal rate

The ablated mass per laser pulse is obtained assuming that the spatial shape of the hole created in all directions is in accordance with the profile measured in a cross-section. By entering profiled data in SolidWorks 3D modeling software and 180-degree rotation of the profile around the central axis, the approximate three-dimensional shape of the cavity and subsequently the approximate volume of the cavity are obtained. Using the relationship $m = \rho \times V$, the volume of the cavity (V) is multiplied by the density of the glass (ρ) to calculate the mass of the material removed. By dividing the mass of the removed material by the number of pulses, the average material removal rate per pulse is obtained. Based on this, the average material removal rate from the glass surface at different laser energies is calculated, and the results are shown in Table 4.

Fig. 7 shows the ratio of the ablation amount with the magnetic field to its amount without the magnetic field for different energies. This ratio at low energies i.e., in the range of copper threshold energy is about 2 to 2.5, but it is increased to about 30 to 35 with an increase in energy.

4- 4- Material spattering:

Regarding material spattering and its deposition on the rear surface of the glass, the samples are drilled under the same conditions with and without the magnetic field. The samples are then imaged by optical microscope, and the results are shown in Fig. 8. It is observed that with the increase of laser energy, the volume of the removed metal material has been increased and consequently the amount of deposited material on the glass has also been increased. Without of magnetic field, the material spattering and metal deposition on the glass and around the inlet of the hole are almost symmetrical, but in a magnetic field presence, the deposition of metal on one side of the hole is greater. Accumulation and deposition of materials on one side of the hole could be due to the way copper ions move in the magnetic field. When a moving charged particle enters a magnetic field, a force field is applied to the charged particle, and the charged particle moves in a circular path. The direction of movement is also determined by the right-hand rule. In this process, copper ions are pulled to one side of the hole for the stated reason. Another possible justification would be that due to the higher temperature of the plasma during the application of the magnetic field and its long life, the particles and components of the plasma hitting the glass surface are molten and after deposition on the glass, the deposited material merges and becomes denser around the hole. This feature can be used in the coating of metals on glass and increase the quality of the metallization.

In Fig. 8, around the created holes wrinkles are observed in wave shape and in the form of concentric circles. These wrinkles are due to the plasma shock waves that hit the glass

Table 4. The material removal rate in various conditions

Condition	Laser Fluence J /cm^2	Avg. ablated mass (n.gr)	Avg. ablated mass per pulse (n.gr)
Without magnetic field	1	0.14	2.8×10^{-3}
	1.5	1.8	3.6×10^{-2}
	3	110.2	2.2
	3.5	224.5	4.5
With magnetic field	1	0.27	5.4×10^{-3}
	1.5	4.4	8.8×10^{-2}
	3	3458.7	69.1
	3.5	7867.8	157.3
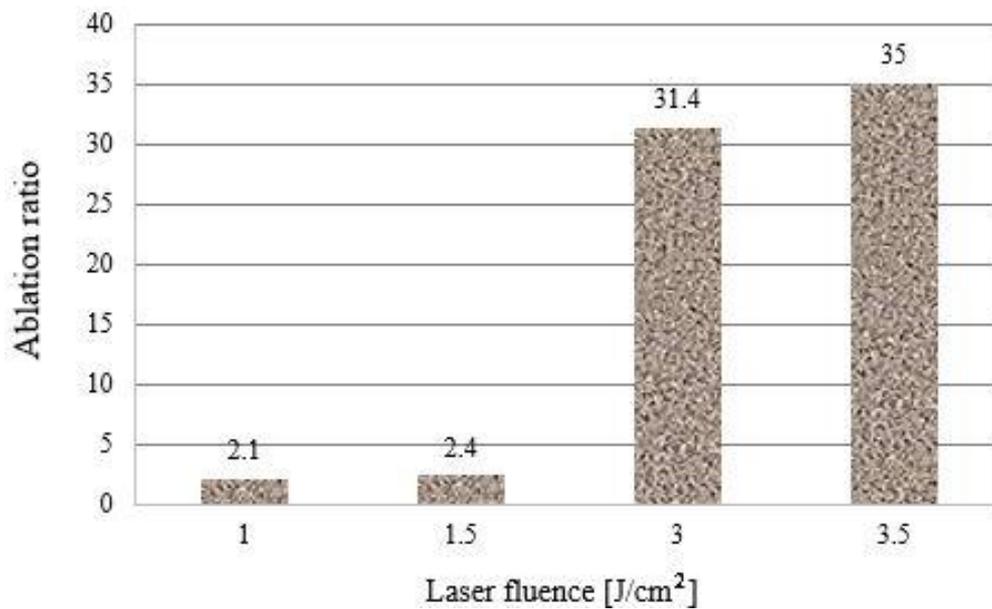
Fig. 7. The ratio of the amount of ablation in the presence of a magnetic field to the amount of ablation in its absence

(a) $E = 1/5$

(b) $E = 3$
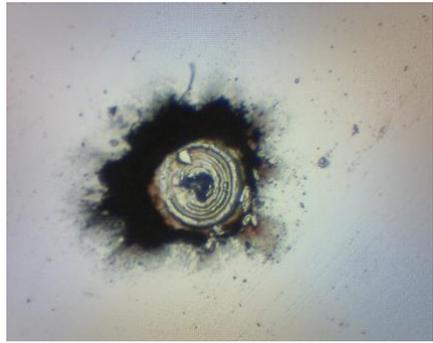
(c) $E = 1/5$
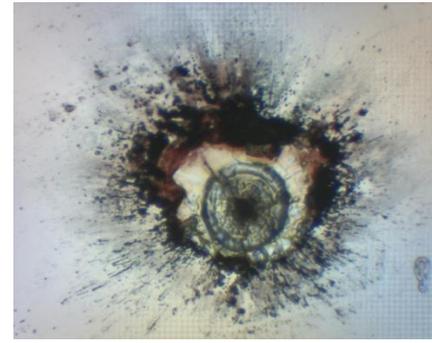
(d) $E = 3$

Fig. 8: Spattering and deposition of molten material around the hole in the E=1/5 and E=3 (J/Cm²) laser fluences a, b) Spattering in the absence of a magnetic field c, d) Spattering in the presence of a magnetic field and orienting the deposition of the material in one side of the hole

surface affecting the area around the entrance to the hole in addition to drilling the glass. A plasma shock wave due to its very high pressure can cause cracks in the entrance of the hole. As the laser energy increases, the plasma pressure increases, and the probability of damage to the workpiece increases. Thus, in machining using this process it is important to select values of the parameters such that these damages are avoided as much as possible.

5- Conclusion:

The main purpose of this study was to investigate the effects of applying a magnetic field on the process of glass ablation with laser-induced plasma. Several experiments on the machining of glass were performed in the presence and absence of a magnetic field. The following results were obtained:

• By applying an external magnetic field, the amount of glass ablation caused by the plasma generated from laser-matter interaction increases.

• As the laser energy increases the magnetic field effect on the plasma increases due to the formation of a larger plasma and the percentage of increase in the rate of ablation increases sharply.

• Material spattering and its condensed deposition on the rear surface of the glass in the magnetic field presence shows the integrity and orientation on one side around the hole which can be used for glass metallization with high quality.

References

[1] M. Kirchhoff, M. Ilg, D. Cote, Application of borophosphosilicate glass (BPSG) in microelectronic processing, Berichte der Bunsengesellschaft für physikalische Chemie, 100(9) (1996) 1434-1437.

[2] K. Li, G. Xu, X. Huang, Z. Xie, F. Gong, Temperature effect on the deformation and optical quality of moulded glass lenses in precision glass moulding, International Journal of Applied Glass Science, 11(1) (2020) 185-194.

[3] Y. Suzuka, M. Ota, Optical device, optical device controller, and method for manufacturing optical device, in, Google Patents, 2020.

[4] A. Crespi, R. Osellame, F. Bragheri, Femtosecond-laser-written optofluidics in alumino-borosilicate glass, Optical Materials: X, 4 (2019) 100042.

[5] E.S. Hamilton, A.R. Hawkins, Direct macro-to-micro interface method for microfluidics, Journal of

Micromechanics and Microengineering, 30(5) (2020) 057001.

[6] Y. Liu, A. Hansen, R.K. Shaha, C. Frick, J. Oakey, Bench scale glass-to-glass bonding for microfluidic prototyping, Microsystem Technologies, (2020) 1-9.

[7] G.C. Rezende, S. Le Calvé, J.J. Brandner, D. Newport, Micro photoionization detectors, Sensors and Actuators B: Chemical, 287 (2019) 86-94.

[8] R. Tölke, A. Bieberle-Hütter, A. Evans, J. Rupp, L. Gauckler, Processing of Foturan® glass ceramic substrates for micro-solid oxide fuel cells, Journal of the European Ceramic Society, 32(12) (2012) 3229-3238

[9] M. Rich, O. Mohd, F.S. Ligler, G.M. Walker, Characterization of glass frit capillary pumps for microfluidic devices, Microfluidics and Nanofluidics, 23(5) (2019) 1-9.

[10] J. Hwang, Y.H. Cho, M.S. Park, B.H. Kim, Microchannel fabrication on glass materials for microfluidic devices, International Journal of Precision Engineering and Manufacturing, 20(3) (2019) 479-495.

[11] S. Kumar, A. Dvivedi, Effect of tool materials on performance of rotary tool micro-USM process during fabrication of microchannels, Journal of the Brazilian Society of Mechanical Sciences and Engineering, 41(10) (2019) 1-16.

[12] M.S. Cheema, A. Dvivedi, A.K. Sharma, Tool wear studies in fabrication of microchannels in ultrasonic micromachining, Ultrasonics, 57 (2015) 57-64

[13] M. Azmir, A. Ahsan, A study of abrasive water jet machining process on glass/epoxy composite laminate, Journal of Materials Processing Technology, 209(20) (2009) 6168-6173.

[14] F. Mehrabi, M. Farahnakian, S. Elhami, M. Razfar, Application of electrolyte injection to the electro-chemical discharge machining (ECDM) on the optical glass, Journal of Materials Processing Technology, 255 (2018) 665-672.

[15] A. Behroozfar, M.R. Razfar, Experimental and numerical study of material removal in electrochemical discharge machining (ECDM), Materials and Manufacturing Processes, 31(4) (2016) 495-503.

[16] M. Hajian, M.R. Razfar, S. Movahed, An experimental study on the effect of magnetic field orientations and electrolyte concentrations on ECDM milling performance of glass, Precision Engineering, 45 (2016) 322-331.

[17] J. Arab, H.S. Chauhan, P. Dixit, Electrochemical discharge machining of soda lime glass for MEMS applications, International Journal of Precision Technology, 8(2-4) (2019) 220-236.

[18] L. Zhang, W. Wang, X.-J. Ju, R. Xie, Z. Liu, L.-Y. Chu, Fabrication of glass-based microfluidic devices with dry film photoresists as pattern transfer masks for wet etching, RSC Advances, 5(8) (2015) 5638-5646.

[19] S. Das, V.C. Srivastava, Microfluidic-based photocatalytic microreactor for environmental application: a review of fabrication substrates and techniques, and operating parameters, Photochemical & Photobiological Sciences, 15(6) (2016) 714-730.

[20] U. Sarma, S.N. Joshi, Effect of Laser Parameters on Laser-Induced Plasma-Assisted Ablation (LIPAA) of Glass, in: Advances in Unconventional Machining and Composites, Springer, 2020, pp. 67-76.

[21] M. Ghoreishi, D. Low, L. Li, Comparative statistical analysis of hole taper and circularity in laser percussion drilling, International Journal of Machine Tools and Manufacture, 42(9) (2002) 985-995.

[22] E. Golchin, M. Moradi, S. Shamsaei, Laser drilling simulation of glass by using finite element method and selecting the suitable Gaussian distribution, in: Modares Mechanical Engineering, Proceedings of the Advanced Machining and Machine Tools Conference, 2015, pp. 416-420

[23] J. Zhang, K. Sugioka, K. Midorikawa, Micromachining of glass materials by laser-induced plasma-assisted ablation (LIPAA) using a conventional nanosecond laser, in: Laser Applications in Microelectronic and Optoelectronic Manufacturing IV, International Society for Optics and Photonics, 1999, pp. 363-369.

[24] G. Kibria, B. Bhattacharyya, J.P. Davim, Non-traditional micromachining processes, Springer, 2017.

[25] J. Zhang, K. Sugioka, K. Midorikawa, Microprocessing of glass materials by laser-induced plasma-assisted ablation using nanosecond pulsed lasers, in: Laser Applications in Microelectronic and Optoelectronic Manufacturing V, International Society for Optics and Photonics, 2000, pp. 332-337.

[26] V.M. Kadan, I.V. Blonsky, V.O. Salnikov, E.V. Orieshko, Effects of laser-induced plasma in machining of transparent materials, in: Micromachining and Microfabrication Process Technology X, International Society for Optics and Photonics, 2005, pp. 130-137.

[27] Y. Hanada, K. Sugioka, Y. Gomi, H. Yamaoka, O. Otsuki, I. Miyamoto, K. Midorikawa, Development of practical system for laser-induced plasma-assisted ablation (LIPAA) for micromachining of glass materials, Applied Physics A, 79(4) (2004) 1001-1003.

[28]]Y. Hanada, K. Sugioka, H. Takase, H. Takai, I. Miyamoto, K. Midorikawa, Selective metallization of polyimide by laser-induced plasma-assisted ablation (LIPAA), Applied Physics A, 80(1) (2005) 111-115.

[29] Y. Hanada, K. Sugioka, K. Midorikawa, Laser-induced plasma-assisted ablation (LIPAA): fundamental and industrial applications, in: High-Power Laser Ablation VI, International Society for Optics and Photonics, 2006, pp. 626111.

[30] S. Xu, B. Liu, C. Pan, L. Ren, B. Tang, Q. Hu, L. Jiang, Ultrafast fabrication of micro-channels and graphite patterns on glass by nanosecond laser-induced plasma-assisted ablation (LIPAA) for electrofluidic devices, Journal of Materials Processing Technology, 247 (2017) 204-213.

[31] T. Rahman, Z. Rehman, S. Ullah, H. Qayyum, B. Shafique, R. Ali, U. Liaqat, A. Dogar, A. Qayyum, Laser-induced plasma-assisted ablation (LIPAA) of glass: Effects of the laser fluence on plasma parameters and crater morphology, Optics & Laser Technology, 120 (2019) 105768.

[32]]Y. Zhao, Q. Li, Z. Wang, Z. Dai, T. Chen, Microchannel fabrication in fused quartz by backside laser-induced plasma ablation using 248 nm KrF excimer laser, Applied Sciences, 9(24) (2019) 5320.

[33] N.B. Dahotre, S. Harimkar, Laser fabrication and machining of materials, Springer Science & Business Media, 2008.

[34] B. Wu, S. Tao, S. Lei, The interactions of microhole sidewall with plasma induced by femtosecond laser ablation in high-aspect-ratio microholes, Journal of manufacturing science and engineering, 134(1) (2012).

[35] S. Harilal, M. Tillack, B. O'shay, C. Bindhu, F. Najmabadi, Confinement and dynamics of laser-produced plasma expanding across a transverse magnetic field, Physical Review E, 69(2) (2004) 026413.

[36] K. Kondo, T. Kanesue, J. Tamura, R. Dabrowski, M. Okamura, Laser plasma in a magnetic field, Review of Scientific Instruments, 81(2) (2010) 02B716.

[37] C. Pagano, J. Lunney, Lateral confinement of laser ablation plasma in magnetic field, Journal of Physics D: Applied Physics, 43(30) (2010) 305202.

[38] k.S. Lash, R. Gilgenbach, C. Ching, Laser-ablation-assisted-plasma discharges of aluminum in a transverse-magnetic field, Applied physics letters, 65(5) (1994) 531-533.

[39] C. Ye, G.J. Cheng, S. Tao, B. Wu, Magnetic field effects on laser drilling, Journal of Manufacturing Science and Engineering, 135(6) (2013).

[40] -J. Chang, C.-L. Kuo, N.-Y. Wang, Magnetic Assisted Laser Micromachining for Highly Reflective Metals, Journal of Laser Micro/nanoengineering, 7(3) (2012).

[41] S. Wolff, I. Saxena, A preliminary study on the effect of external magnetic fields on laser-induced plasma micromachining (LIPMM), Manufacturing Letters, 2(2) (2014) 54-59.

[42] R. Fabbro, J. Fournier, P. Ballard, D. Devaux, J. Virmont, Physical study of laser-produced plasma in confined geometry, Journal of applied physics, 68(2) (1990) 775-784.

[43] K.A. Pathak, A.J. Chandy, Laser ablated carbon plume flow dynamics under magnetic field, Journal of Applied Physics, 105(8) (2009) 084909.

[44] Y.T. Lee, R. More, An electron conductivity model for dense plasmas, The Physics of fluids, 27(5) (1984) 1273-1286.

[45] S. Elhami, M. Razfar, Study of the current signal and material removal during ultrasonic-assisted electrochemical discharge machining, The International Journal of Advanced Manufacturing Technology, 92(5) (2017) 1591-1599.